IJNRD.ORG ISSN : 2456-4184
INTERNATIONAL JOURNAL OF NOVEL RESEARCH AND DEVELOPMENT (IJNRD) | IJNRD.ORG
An International Open Access, Peer-reviewed, Refereed Journal

Lineament Extraction In Olkaria Geothermal Field Using Sentinel-1A imagery (Kenya).

Esther Waithera Githinji

Student Master of Science in Geothermal Sciences of the Jomo Kenyatta University of Agriculture and Technology

Supervisors.

Prof. John Githiri

Department of Physics, Jomo Kenyatta University of Agriculture and Technology.

Dr. Mercy Mwaniki

Department of Geomatics Engineering and Geospatial Information Systems, Jomo Kenyatta University of Agriculture and Technology.

ABSTRACT

Subsurface processes are displayed as observable ground deformations. Their identification and monitoring provide insight about Earth's dynamics and processes triggering these conditions. This paper aims to show the application of remote sensing technique in obtaining preliminary information about the subsurface through extraction of geological lineaments in the middle fault zone of the Olkaria geothermal field. The Olkaria West Field (OWF) and East fields are separated by a low-temperature zone; waters from the west field fracture have lower enthalpy. Further, the wells on either side show different reservoir fluid characteristics. In this study, Sentinel-1 Synthetic Aperture Radar (SAR) imagery was used. Image analysis techniques used were Gray Level Co-occurrence Matrix (GLCM) for texture analysis and Line module algorithms for edge detection to obtain the tectonic lineaments. The rose diagrams were used to display the lineaments' orientation. The main trends observed in the lineament map for the zone between East and West fields could be recognized as showing a major trend in S-N, this orientation might be correlated with the fractured volcanic system of Olkaria Geothermal field. Detection of geologic lineaments using free Sentiel-1 data presents a great advantage for future geological surveys.

Key words: Sentinel-1, Gray level, Lineaments

INTRODUCTION

Remote Sensing of the earth's surface records energy reflected or radiated by an object at different wavelengths of the electromagnetic (EM) spectrum. It allows identification of geological structures on the surface and interpretation of geophysical surveys allows interpretation of their continuity in the subsurface. Sentinel-1 Synthetic Aperture Radar (SAR) allows precise coverage of vast regions in less time with basic data for geological exploration while significantly reducing costs. The data provides valuable mapping information as an exploration tool for mineral and petroleum, environmental assessment as well and geothermal development(Chaabouni, 2012)

RS work done before at Olkaria Geothermal Field used thermal images Landsat TM band 6 for geothermal mapping, to determine geophysical characteristics of volcanoes, hot springs and locate geologic faults(Pastor, 2010). Further Kenya's lineament map from Landsat images in correlation to known geological data was mapped with lithological boundaries, mineral locations and zones of micro-seismics within the rift zone (Gaciri, 1992). A combination of remote sensing and geophysical techniques has proved successful, for example gravity and remote sensing were used to identify geological structures in Indonesia(Darmawan et al., 2021).

This study used automatic lineament extraction using computer software and algorithms. The most widely used software is the line module of the PCI Geomatica. Detection and quantification of displacements due to tectonics represent an important task for the understanding of Earth's surface and subsurface dynamics. Changes through differential interferometry by making use of SAR is the approach of this study (Necula et al., 2018).

This technique relies on the exploitation of signal phase property which allows measurement of terrain changes. Geological structural lineaments and their orientation in the middle fault zone of the Olkaria geothermal field were obtained to provide basic information that could result ground deformations leading to different reservoir characteristics between the East and the West fields (Wamalwa et al., 2016).

Study area

Olkaria Geothermal Field lies approximately 122 kilometers by road, northwest of Nairobi, in Olkaria ward Nakuru County (Figure 1). It is structurally controlled and dominated by faults, fissures, volcanic centers, and domes, among others. The main tectonic structures in the Olkaria volcanic complex include fractures, faults, the Ol'Njorowa gorge, and the ring structure (Okoo et al., 2017).

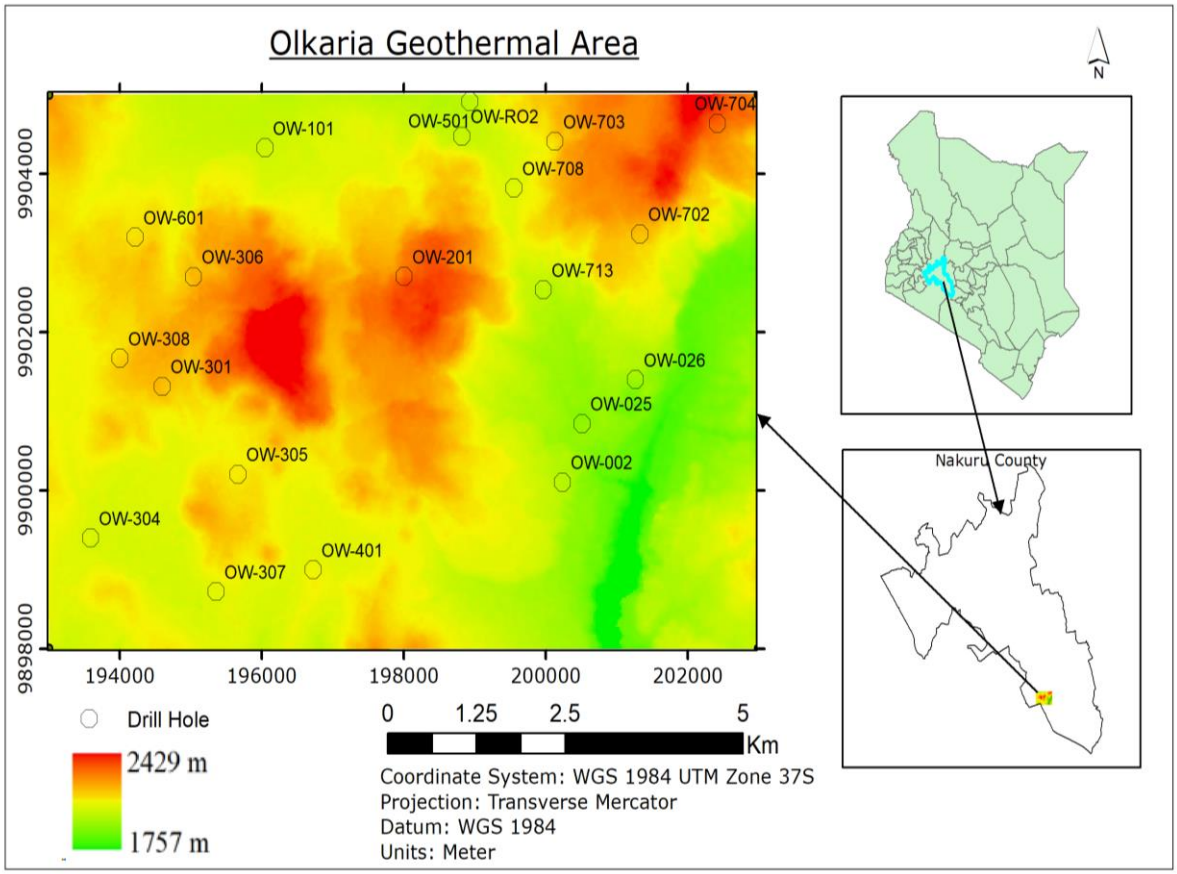

Figure 1: Location of the Olkaria Geothermal area in Nakuru County Kenya

Geology of study area

Olkaria is a high-temperature geothermal system located within the central sector of the Kenya Rift Valley and associated with an area of late Quaternary rhyolitic volcanism (Figure *2*). The geology is dominated by Pleistocene-Holocene, Holocene comenditic rhyolite flows on the surface and basalts, trachytes, and tuffs in the subsurface. The Olkaria field can be separated into east and west stratigraphic zones with the divide through the Olkaria Hill (Otieno, 2012).

The reservoir characteristics also follow this zonation. The geothermal reservoir in the east is hosted within Pleistocene Plateau Trachytes, while in the west it is within the Pliocene Mau Tuffs. Structural, geochemical, and hydrothermal alteration patterns indicate that the west field is at the margin of the larger Olkaria system. The anomalous bicarbonate enrichment in the west sector is due to additional adsorbed carbon dioxide from the mantle (Omenda, 1998).

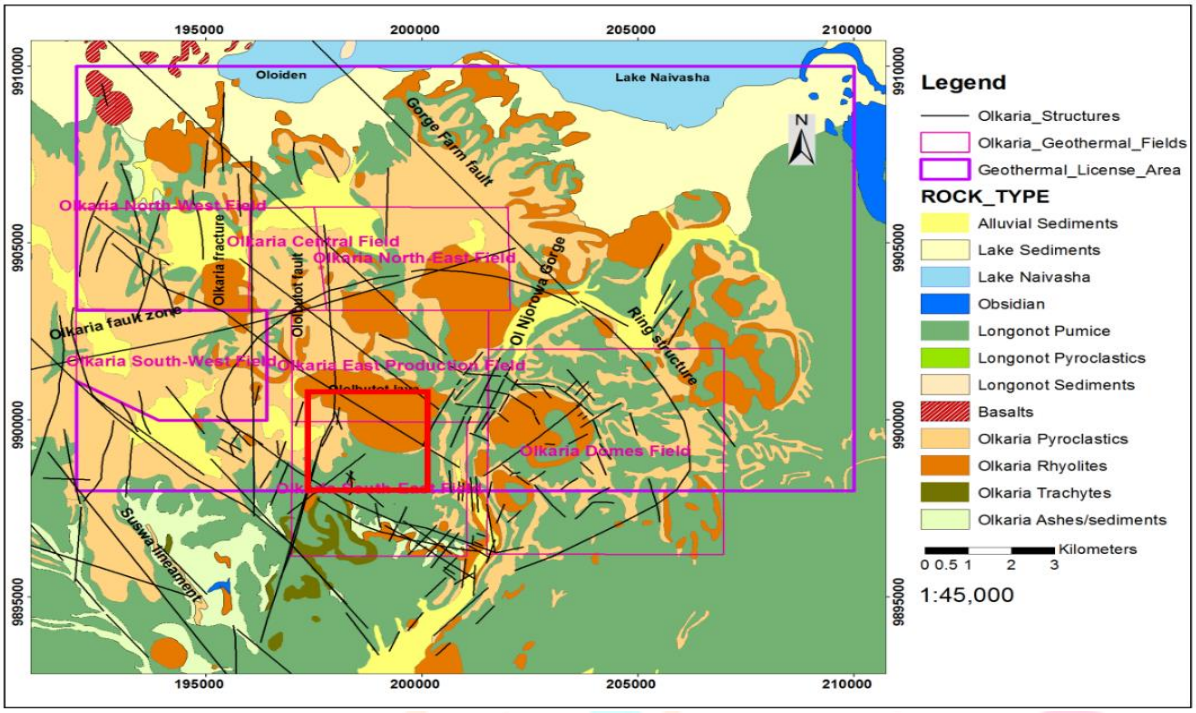

Figure 2: Surface geology and structures in the Greater Olkaria geothermal area (Ngetich, 2018)

METHODOLOGY

Data

Sentinel-1 image was downloaded from the European Space Agency (ESA) data hub https://scihub.copernicus.eu/dhus/ and was subset to match with the extent of the study area in SNAP software, specifications of the imagery displayed in (Figure 3). SNAPv6.0 software was developed by the Department of Geodesy and Geoinformation at the TU Wien. It is largely used for processing Sentinel-1 products in the extraction of geophysical parameters (Bauer-Marschallinger et al., 2021).

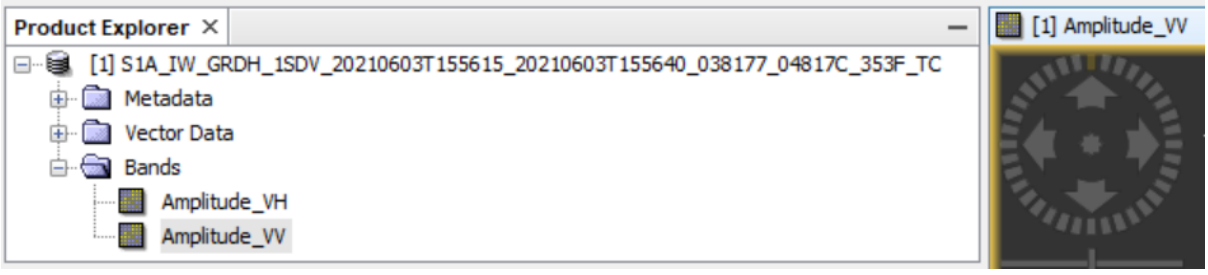

Figure 3 Sentinel-1 Image specifications

Workflow

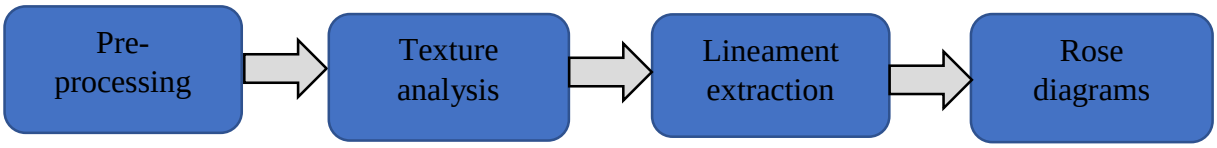

Figure 4: Research Flow Chart

Image pre-processing

Sub-setting and calibration of the SAR were performed to provide an image in which the pixel values were directly related to the radar backscatter of the scene by use of the SNAP software. The image was imported to the software (Figure 5). The band VV subset Spatial, the points grid was checked, Metadata conversion and the image was saved as a subset.

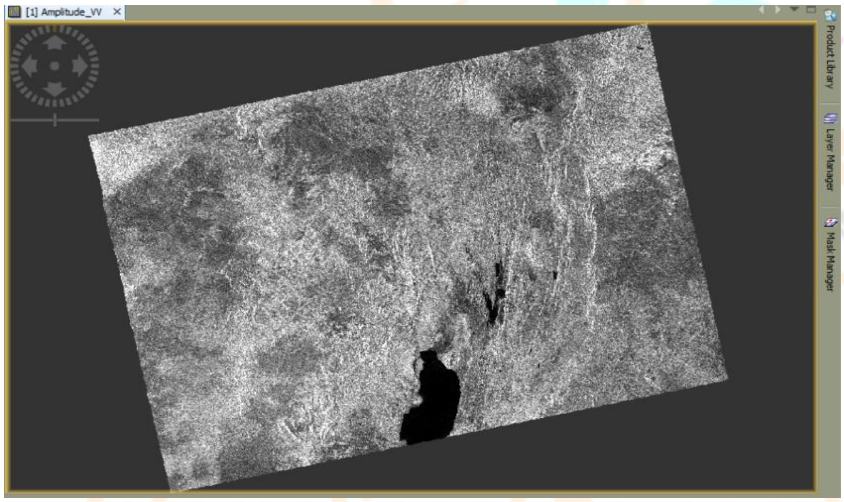

Figure 5: Sentinel-1A GRDH dataset in IW from SNAP software

Geo-referencing which involved matching the Sentinel-1 radar image with the image on the ground was done automatically with the snap software, where coordinates from the Olkaria map as well as the location of the wells were used as ground control points (GCP).

Ground control points (UTM coordinates)

Range Doppler terrain	1	193000	9905000
	2	203000	9905000
	3	193000	9898000
	4	203000	9898000

correction was done to correct geometric distortions caused by topography using WSG 1984 datum and was the final step of processing the SAR.

Texture analysis

The Gray Level Co-occurrence Matrix (GLCM) method from SNAP software was used to compute features such as contrast, entropy, homogeneity, dissimilarity and energy. Angular spatial and distance relationships among grey levels of remotely sensed data are summarized in the GLCM. It is the measure of the probability of the occurrence of two gray levels separate by a given distance in a given direction (Kuplich, 2017).

Texture measures analyzed in this work are presented below, in all the formulas p(i;j) stands for (i;j)th entry where i and j are the horizontal and vertical cell coordinates and p is the cell value in a normalized GLCM. Contrast is a local grey level variation in the grey level co-occurrence matrix, the linear dependency of grey levels of neighboring pixels (Eqn1). Homogeneity measures the uniformity of the non-zero entries in the GLCM. It weights values by the inverse of contrast weight (Eqn2) (Gebejes et al., 2013).

Entropy is the measure of the degree of disorder in an image (Eqn3). Dissimilarity is a measure that defines the variation of grey-level pairs in an image (Eqn4). Energy is a measure of local homogeneity and therefore it represents the opposite of the Entropy. This feature will tell us how uniform the texture is (Eqn5) (Gebejes et al., 2013).

$$Contrast = \sum_{i,j} | i - j |^2 \, p(\mathrm{i},\mathrm{j}) \tag{1}$$

$$Homogeneity = \sum_{i,j} \frac{1}{1-(i-j)^2} p(\mathrm{i},\mathrm{j}) \tag{2}$$

$$Entropy = -\sum_{i,j} p(\mathrm{i},\mathrm{j}) log(p(\mathrm{i},\mathrm{j}) \tag{3}$$

$$Dissimilarity = \sum_{i,j} | i - j \, | \, 2p(\mathrm{i},\mathrm{j}) \tag{4}$$

$$Energy = \sum_{i,j} p(i,j)^2 \tag{5}$$

Lineaments' extraction

After texture analysis, the image was saved as a geotiff and the LINE module algorithm of PCI Geomatica software was used to extract linear features from the raster image (Javhar et al., 2019). The algorithm consists of six parameters grouped mainly as edge detection and, curve extraction and thresholding which give output as vector segments (Sedrette & Rebaï, 2016).

Edge detection and thresholding consist of filter Radius (RADI), a Gaussian filter radius used during the edge detection, measured in pixels; with recommended values between 3–8 and the Edge Gradient Threshold (GTHR) which is the minimum value of gradient to be considered as an edge during the edge detection with accepted values between 10–70 (Javhar et al., 2019).

Curve extraction and thresholding have four parameters. Curve Length Threshold (LTHR) is the minimum length of a curve to be considered as a lineament with the common value of 10 in most cases. Line Fitting Error Threshold (FTHR) is the maximum error allowed during the line segment fitting to form a lineament with the recommended values between 2–5, Angular Difference Threshold (ATHR), specifies the angle not to be exceeded between two vectors to be linked with the suitable angle between 3 to 20 degrees (Ahmadi et al., 2021).

Lastly, the Linking Distance Threshold (DTHR), is the maximum distance between two vectors to be linked. The lineaments were analyzed to extract information related to length and orientation analysis with the aid of rose diagrams (Farahbakhsh et al., 2020).

RESULTS AND DISCUSSION

The availability of high-resolution multispectral data and the ability of digital image processing techniques of SAR enables efficient and quick extraction of geological lineaments extraction with greater accuracy more so allowing identification of lineament features that are occluded by the vegetation cover that are imperceptible in the optical data (Chaabouni, 2012).

Lineaments in the entire Olkaria Geothermal Field were extracted from the Sentinel-1 dataset using the LINE module of Geomatica software (Figure 6). The rose diagrams suggested NE-SW, NNE-SSW, N-S, NNW-SSW, and NW-SE lineaments orientation (Figure 7). Lineaments obtained from this research concur with earlier findings that greater Olkaria geothermal field structures include ENE-WSW, N-S, NNE-SSW, NW-SE and WNW-ESE trending faults (Wamalwa et al., 2016).

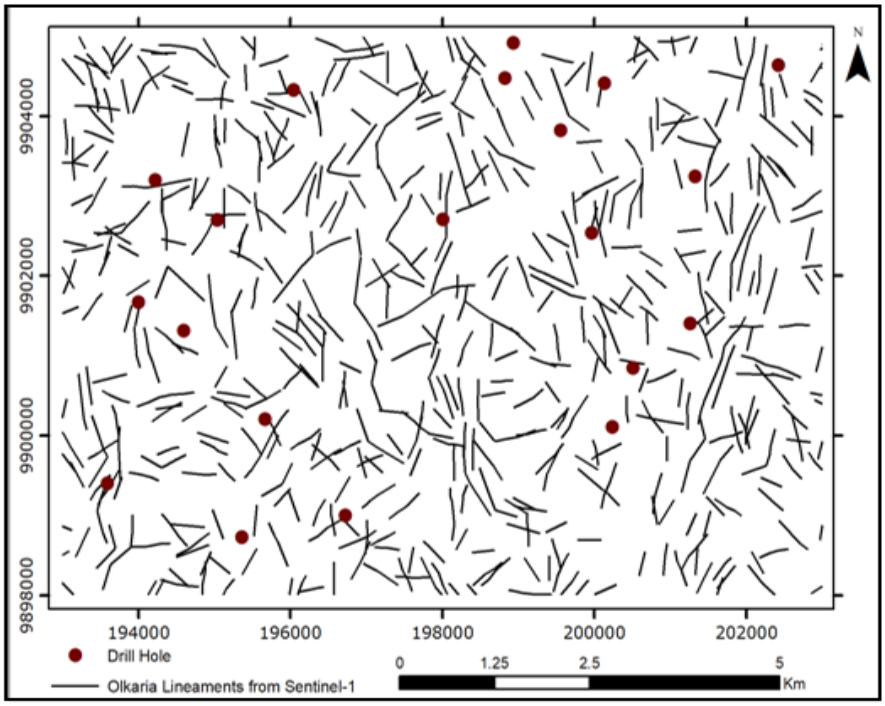

Figure 6 Olkaria Geothermal Field Sentinel-1A GRDH VV polarization lineaments

.

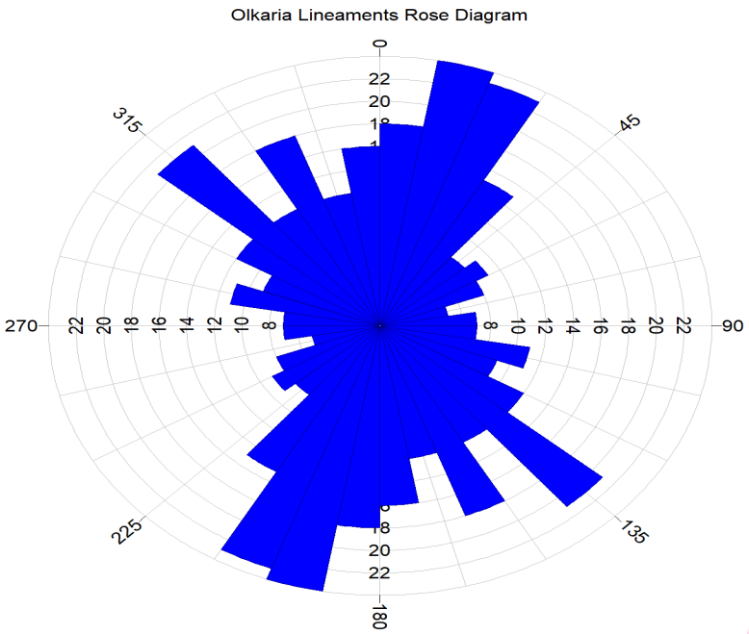

Figure 7: Rose diagram for the entire Olkaria Geothermal area

Fracturing of the subsurface leads to linear structural geology where straight lineaments are grouped as tertiary lineaments; the small and shallow, secondary lineaments; medium length and depth or main lineaments; long and deep, and the intersection of different lineaments act as a guide to the faulting planes, where faults are known to leading to different reservoir characteristic(Chaabouni, 2012).

Investigations show that most prominent geothermal sites have been found in the vicinity of active fault system and fault intersections host appropriate physical settings for these geothermal sites, as permeability and fluid flow is substantially enhanced at this sports(Geowissenschaften, 2015). The NE-SW trending Olkaria fracture tends to carry cool temperature waters with low chlorine content that have led to a decline in enthalpies of the wells it cuts through while NW-SE trending faults bring in high temperature and Chlorine rich waters(Wamalwa et al., 2016).

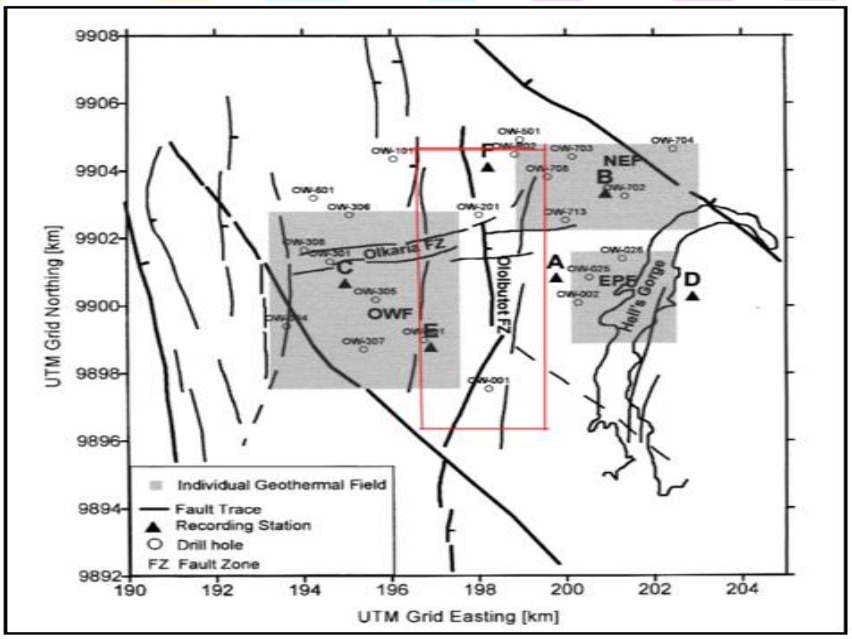

Figure 8: Olkaria faults, middle-fault zone area in red

In this study, more emphasis was put on the central Olkaria zone to establish whether there is a major fracturing along the North-South between the East and West fields (Figure 8). Sentinel-1 SAR lineaments analysis established the existence of lineaments majorly in N-S orientation as indicated by the rose diagram () when compared with the orientation of lineaments of the entire Olkaria zone. DEM (Digital Elevation Model) of Olkaria Geothermal field displaying the middle-fault zone lineaments extracted (Figure 9).

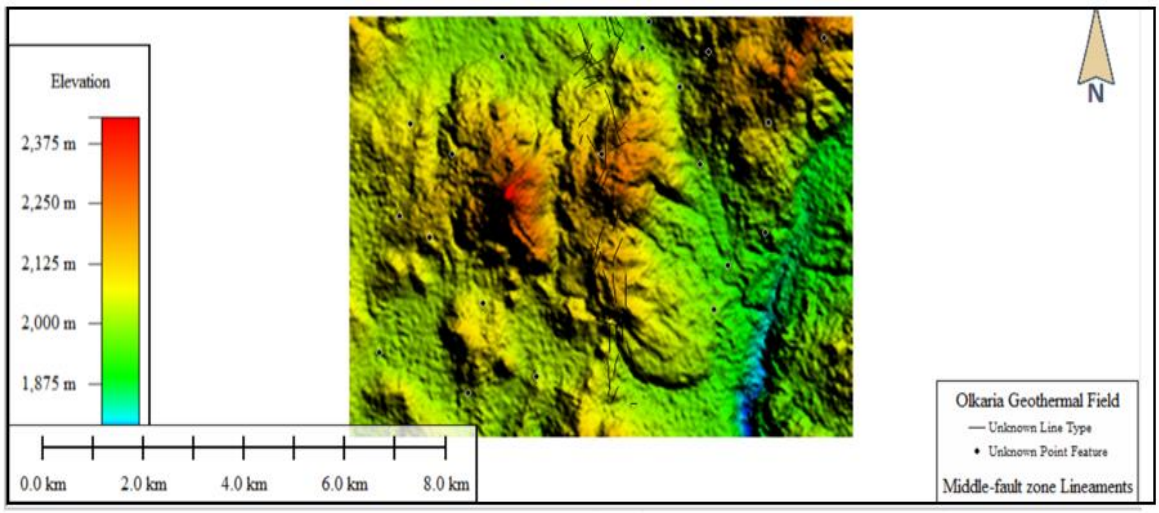

Figure 9: DEM of Olkaria Geothermal area with the lineaments of the middle fault zone

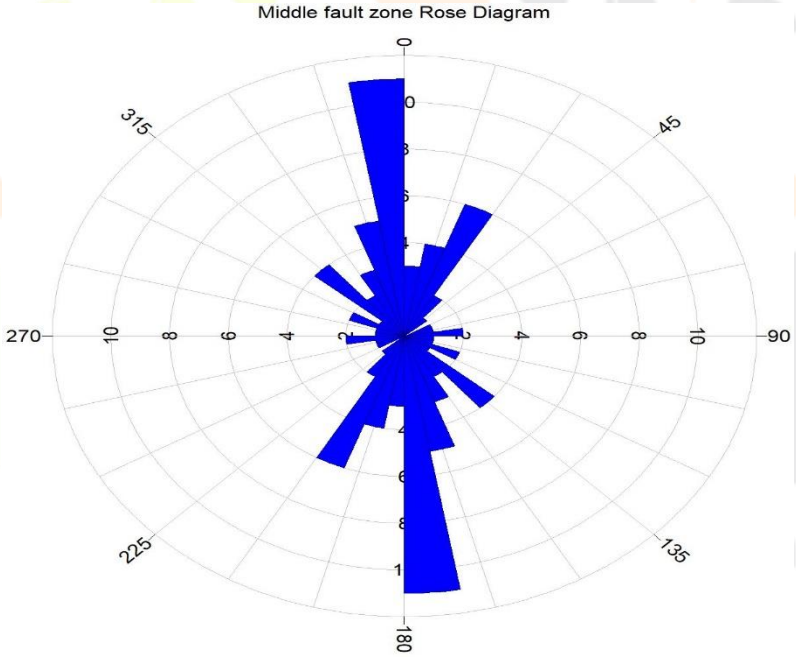

Figure 10 Rose diagram for the middle fault zone

CONCLUSION

In this paper, an attempt has been made to map lineaments and knowledgebase preparation using geomatics techniques and expert systems for part of the Olkaria region. Sentinel-1A SAR was analyzed for automatic

lineaments extraction under parameter values within the LINE module of PCI Geomatica software. According to digitalized lineaments extracted from the geological map of the Olkaria, the rose diagrams compare the extent of the orientation of the lineaments. The result of this study shows a positive correlation between structural geology and the extracted faults orientation. Directional peaks recorded are consistent with the results of previous work undertaken in the Olkaria region. However central zone proved to have faults aligned in the N-S direction that could have been overlooked.

To conclude, we can note that automatic extraction of lineaments is a useful way to delineate lineaments for different purposes, such as defining geological structures as this offers preliminary information that will guide the other subsurface techniques.

REFERENCES

Ahmadi, H., Pekkan, E., & Martinez-Frias, J. (2021). *geosciences Fault-Based Geological Lineaments Extraction Using Remote Sensing and GIS-A Review*. https://doi.org/10.3390/geosciences11050183

Bauer-Marschallinger, B., Cao, S., Navacchi, C., Freeman, V., Reuß, F., Geudtner, D., Rommen, B., Vega, F. C., Snoeij, P., Attema, E., Reimer, C., & Wagner, W. (2021). The normalised Sentinel-1 Global Backscatter Model, mapping Earth's land surface with C-band microwaves. *Scientific Data*, *8*(1), 1–18. https://doi.org/10.1038/s41597-021-01059-7

Chaabouni, R. (2012). Lineament analysis of South Jenein Area (Southern Tunisia) using remote sensing data and geographic information system. *The Egyptian Journal of Remote Sensing and Space Sciences*, *15*(2), 197–206. https://doi.org/10.1016/j.ejrs.2012.11.001

Darmawan, D., Daud, Y., & Iskandar, C. (2021). Identification of Geological Structure Based on Gravity and Remote Sensing Data in "x" Geothermal Field. *AIP Conference Proceedings*, *2320*(March). https://doi.org/10.1063/5.0038807

European Space Agency, Copernicus Open Access Hub. Retrieved June, 03, 2021 from https://scihub.copernicus.eu/dhus/

Farahbakhsh, E., Chandra, R., Olierook, H. K. H., Scalzo, R., Clark, C., Reddy, S. M., & Müller, R. D. (2020). Computer vision-based framework for extracting tectonic lineaments from optical remote sensing data. *International Journal of Remote Sensing*, *41*(5), 1760–1787. https://doi.org/10.1080/01431161.2019.1674462

Gebejes, A., Master, E. M., & Samples, A. (2013). *Texture Characterization based on Grey-Level Co-occurrence Matrix*. 375–378.

Geowissenschaften, P. (2015). *The role of fault zones on structure, operation and prospects of geothermal reservoirs A case study in Lahendong, Indonesia*.

Javhar, A., Chen, X., Bao, A., Jamshed, A., Yunus, M., Jovid, A., & Latipa, T. (2019). *Remote sensing*

Comparison of Multi-Resolution Optical Landsat-8, Sentinel-2 and Radar Sentinel-1 Data for Automatic Lineament Extraction: A Case Study of Alichur Area, SE Pamir. *11*, 778. https://doi.org/10.3390/rs11070778

Kuplich, T. M. (2017). *Temporal, spatial, spectral and polarisation characteristics of the SAR backscatter from regenerating tropical forests Tatiana Mora*. *December 2001*.

Necula, N., Niculita, M., & Floris, M. (2018). Using Sentinel-1 SAR data to detect earth surface changes related to neotectonics in the Focșani basin (Eastern Romania). *PeerJ Preprints*, 2–5.

Ngetich, E. R., & Box, P. O. (2018). *Mapping of Olkaria Intrusives by Integration of Geologic and Geophysical Techniques*.

Okoo, J., Omiti, A., Kamunya, K., & Saitet, D. (2017). Updated conceptual model of Olkaria geothermal Field Naivasha, Kenya. *Transactions - Geothermal Resources Council*, *41*(Figure 1), 1536–1553.

Omenda, P. A. (1998). The geology and structural controls of the Olkaria geothermal system, Kenya. *Geothermics*, *27*(1), 55–74. https://doi.org/10.1016/S0375-6505(97)00028-X

Otieno, A. B. (2012). *Investigations Into the Permeability and Tectonic*.

Pastor, M. S. (2010). Application of Thermal Remote Sensing for Geothermal Mapping, Lake Naivasha, Kenya. *Proceedings World Geothermal Congress*, *April*, 25–29.

Sedrette, S., & Rebaï, N. (2016). Automatic extraction of lineaments from Landsat Etm+ images and their structural interpretation: Case Study in Nefza region (North West of Tunisia). *Journal of Research in Environmental and Earth Sciences*, *August*, 139–145. http://earthexplorer.usgs.gov.

Wamalwa, R. N., Nyamai, C. M., Ambusso, W. J., Mulwa, J., & Waswa, A. K. (2016). Structural Controls on the Geochemistry and Output of the Wells in the Olkaria Geothermal Field of the Kenyan Rift Valley. *International Journal of Geosciences*, *07*(11), 1299–1309. https://doi.org/10.4236/ijg.2016.711094